

Albert Hofmann, Kurt Hübner and Bruno Zotter \*

Abstract

A computer program is presented which assists the designer of a circular electron accelerator or storage ring in finding out the limits of beam stability. The most prominent longitudinal and transverse instabilities are taken into account with emphasis on coherent bunch oscillations.

1. Introduction

The program calculates parameters, thresholds and growth rates for various effects known to affect the stability of high-intensity electron beams. Generally it does not endeavour to find equilibrium conditions after an instability has occurred, and it neglects coupling between the individual effects. Only single beam stability is treated; beam-beam effects are not considered. The program is based on currently accepted models of beam stability, most of them confirmed by experiments. The FORTRAN code and a long write-up can be obtained from the authors. A numerical example, based on the parameters of the Large Electron-Positron storage ring LEP<sup>1</sup> is presented at the end.

2. Impedance Estimates

Most of the models require a detailed knowledge of the impedance versus frequency. Three types of impedance are considered: i) a typical high-Q resonator is used to assess the disturbance it might present to the beam if one of the beam frequencies happens to fall into its narrow bandwidth; ii) a broad band impedance approximates the effect of a multitude of individual high-Q resonators on single-bunch phenomena; iii) the impedance of the smooth resistive vacuum chamber is expected to have an influence mainly on single-bunch phenomena due to its peculiar frequency dependence ( $\omega^{-2}$ ), though it contributes also to multi-turn effects.

2.1 Longitudinal impedance

The relevant quantity is the complex impedance  $Z_L$  divided by the mode number  $r = \omega/\omega_0$  ( $\omega_0$  - circular revolution frequency). For a resonator, approximated by a parallel RLC circuit, this quantity becomes, with  $Q_R$  as quality factor,

$$\frac{Z_{LRES}}{r} = \frac{R_S \omega_0}{\omega_r} \frac{(\omega/\omega_r) + jQ_R(1 - (\omega/\omega_r))}{(\omega/\omega_r)^2 + Q_R^2(1 - (\omega/\omega_r)^2)^2} \quad (1)$$

It is plotted versus frequency in Fig. 1a. High-Q resonators drive instabilities involving the bunches passing during the time  $2\pi Q_R/\omega_r$ , e.g. coupled-bunch and Robinson instabilities. The RF cavities, including their higher modes, are the most prominent source for this type of impedance which can be computed by standard programs<sup>2,3</sup>. The broad-band impedance, being the source of the short-range wake field, creates oscillations of a single bunch, turbulent bunch-lengthening and real frequency shifts. This impedance is due to aperture changes, bellows and numerous other objects, each resonating at a different frequency. For coherent bunch oscillation, we approximate it by a resonator with  $Q_R = 1$ , having a resonance frequency  $\omega_r$  which we choose to be about half of the cut-off frequency of the lowest longitudinal mode in the vacuum chamber. The shunt impedance  $R_S$  of this resonator can be estimated by forming the limit  $\lim_{\omega \rightarrow 0} |Z_{LRES}/r| = |Z/r|_0 = R_S \omega_0/\omega_r$  which

depends only on the amount of impedance per unit length of the ring and not on the size of the machine. For the older machines  $|Z/r|_0$  is in the range 10 to 50  $\Omega$ , for modern machines with smooth vacuum chambers such as PETRA and PEP it is considerably smaller. For turbulent bunch lengthening, the broad-band impedance is approximated by  $Z_L/r = \text{const}$  at low frequencies and by  $Z_L/r \sim \omega^{-a}$  ( $0 < a < 1$ ) at high frequencies, because such an impedance has been inferred from the measurements in SPEAR<sup>4</sup>. The impedance of the smooth, resistive wall of the vacuum chamber is neglected against the broad-band impedance in the longitudinal case.

2.2 Transverse impedance<sup>5</sup>

In order to obtain the narrow-band transverse impedance the deflection modes of cavity-like objects have to be computed<sup>6</sup>. The transverse impedance  $Z_T$  of a narrow-band resonator has the same form as (1) except that  $R_S \omega_0/\omega_r$  is replaced by  $R_T$ . The broad-band impedance can be estimated from the longitudinal one by using the relation<sup>7</sup>

$$Z_T(\omega) \approx (2R/b^2) \cdot (Z_L(\omega)/r) \quad (2)$$

where  $b$  is the effective radius<sup>8</sup> of the vacuum envelope around the beam; it is equal to the radius for objects with circular cross-sections.  $R$  is the average radius of the machine. The relation (2) has to be applied separately to objects with large radius  $b$  (cavities) and to items with small  $b$  (bellows etc.). The total  $Z_T$  is then the sum of the two contributions. The relative contribution of the RF cavities to the total transverse impedance will be smaller than to the longitudinal one. Equation (2) indicates that the transverse impedance is proportional to the machine radius  $R$  because  $Z_L/r$  is approximately independent of  $R$  as explained before. Hence, transverse stability becomes more critical in large machines. The impedance of the smooth, resistive pipe is brought about by the skin effect<sup>5</sup>.

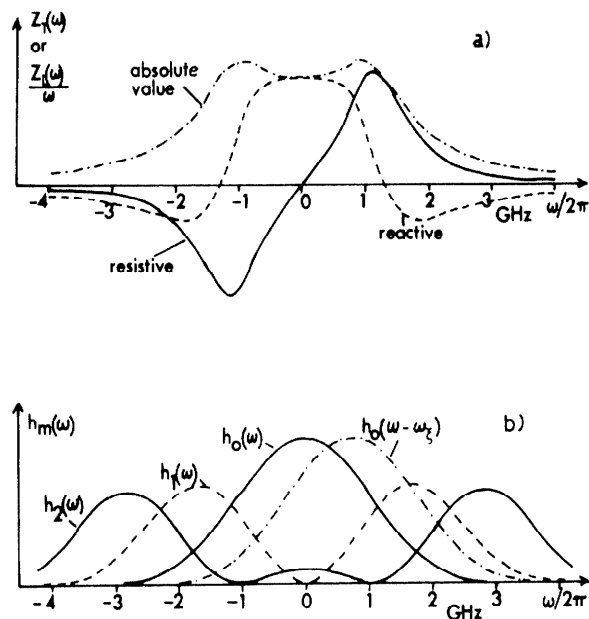


Fig. 1. a) Impedance of a resonator having  $Q_R = 1$ ; b) Envelope of power spectrum  $h_m(\omega)$  for sinusoidal modes.

\* CERN, Geneva, Switzerland

### 3. Particle Distributions and Modes of Oscillation

Coherent bunch oscillations can be described by two independent types of mode: the bunch-shape modes describing the distortion of the bunch itself and the coupled-bunch modes describing the motion of the different bunches relative to each other. The longitudinal-shape modes<sup>9</sup> consist of the dipole (rigid-bunch) mode ( $m = 1$ ), the quadrupole mode ( $m = 2$ ) etc.; in the transverse case, the different head-tail<sup>5</sup> modes describe the shape oscillations, labelled by the number of nodes  $m$  of the perturbed motion. The coupled-bunch modes are labelled with  $n = \Delta\phi \cdot k_b / (2\pi)$  where  $\Delta\phi$  is either the momentary synchrotron or betatron phase advance of one bunch relative to the next one, and  $k_b$  is the number of bunches.

The undisturbed long. distribution is Gaussian with an instantaneous current  $I(t)$

$$I(t) = I_p \exp(-c^2 t^2 / 2\sigma_s^2) = (\sqrt{2\pi} R I_0 / k_b \sigma_s) \exp(-c^2 t^2 / 2\sigma_s^2) \quad (3)$$

where  $\sigma_s$  is the rms bunch length. The instantaneous perturbed current is made up of the contribution of all modes

$$I(t) = \sum_{m,n} C_m \lambda_m \exp(j(\omega_p + \Delta\omega)t) \quad (4)$$

In the limit of vanishing intensity the spectrum consists of lines at frequencies

$$\omega_p = \omega_0 (k \cdot k_b + n + m Q_s) = \omega_0 (p + m Q_s) \quad (5)$$

in the longitudinal case<sup>10</sup>, and

$$\omega_p = \omega_0 (k \cdot k_b + n + Q) = \omega_0 (p + Q) \quad (6)$$

in the transverse case<sup>5</sup>. The constants are  $k = 0, \pm 1, \pm 2, \dots$ ;  $n = 0, 1, 2 \dots k_b - 1$ ;  $Q_s$  is the synchrotron and  $Q$  the betatron tune.

The longitudinal bunch-shape modes are approximated by sinusoidal modes

$$\lambda_m(t) = \begin{cases} \cos \left[ (m+1) \cdot (ct/\sigma_s) \right] & \text{for } m - \text{even} \\ \sin \left[ (m+1) \cdot (ct/\sigma_s) \right] & \text{for } m - \text{odd} \end{cases} \quad (7)$$

though the real modes<sup>11</sup> seem to be between sinusoidal and Hermitian modes. For the computation of coherent frequency shifts the power spectrum  $h_m(\omega)$  of these modes is needed<sup>5,12</sup>. Its envelope is shown in Fig. 1b. For the transverse perturbation (the head-tail modes), the same sinusoidal modes are used with a modification to take into account the effect of finite chromaticity  $\xi = (dQ/Q)/(dp/p)$ <sup>5</sup>. This shifts the mode spectrum by  $\omega_\xi = \xi \cdot Q \cdot \omega_0 \cdot \gamma_t^2$ , and  $h_m(\omega - \omega_\xi)$  must be used in the transverse case as indicated in Fig. 1b. ( $\gamma_t$  is the Lorentz factor at transition energy).

### 4. Coherent Bunch Instabilities

The impedance produces a complex frequency shift  $\Delta\omega$  of the frequency  $\omega_p$  defined by (5) and (6). The real part  $\Delta\omega_R$  gives the coherent frequency shift of the mode ( $m, n$ ) due to the reactive impedance while the imaginary part  $\Delta\omega_I$  gives the damping rate (if  $\Delta\omega_I > 0$ ). The longitudinal frequency shift<sup>12</sup> is

$$\Delta\omega_{mn} = j \frac{m \omega_s}{m+1} \frac{8 I_0}{3 k_b h v \cos \phi_s} \left( \frac{R}{\sigma_s} \right)^3 \left( \frac{Z_L}{r} \right)_{mn}^{eff} \quad (8)$$

where  $\omega_s$  - circular synchrotron frequency,  $h = \omega_{TR}/\omega_0$ ,  $V \sin \phi_s$  - energy gain of synchronous particle. The effective longitudinal impedance<sup>12</sup> is

$$\left( \frac{Z_L}{r} \right)_{mn}^{eff} = \frac{\sum_k Z_L(\omega_p) h_m(\omega_p)/\omega_p}{\sum_k h_m(\omega_p)} \quad (9)$$

where  $\omega_p$  is given by (5). The transverse frequency shift<sup>5</sup> is

$$\Delta\omega_{mn} = j \frac{e c I_0}{(m+1) 2\pi Q k_b E} \left( \frac{R}{\sigma_s} \right) \left( Z_T \right)_{mn}^{eff} \quad (10)$$

with E-beam energy, and the effective transverse impedance<sup>5</sup>

$$\left( Z_T \right)_{mn}^{eff} = \frac{\sum_k Z_T(\omega_p) h_m(\omega_p - \omega_\xi)}{\sum_k h_m(\omega_p - \omega_\xi)} \quad (11)$$

with  $\omega_p$  given by (6). For a coupled bunch mode  $n$  the summation is only over every  $k_b$ th mode. However, all frequencies contribute to the frequency shift  $\Delta\omega_m$  of the single-bunch modes

$$\Delta\omega_m = (1/k_b) \sum_{n=0}^{k_b-1} \Delta\omega_{mn} \quad (12)$$

Equations (8) and (10) give the frequency shifts for all coherent bunch instabilities in the limit of  $|\Delta\omega|$  being small compared to the bandwidth of the resonator. It turns out that the sums (9) and (11) converge very slowly for the reactive part. Fortunately, the sums can be replaced by an analytical expression<sup>13</sup> and this is used in the program.

For the impedance of the smooth resistive wall<sup>5</sup> no such expression is available and the straightforward summation must be carried out. This is done in the code but only up to the lowest cut-off frequency of the pipe. In this crude way the diminishing influence of frequencies in the propagating range is taken into account. For the same reason, the computation is limited to the modes  $m = 0, 1$ . Higher modes have a spectrum entirely in the propagating region of the pipe where the coupling to the beam is weak. The part of the code performing the summing uses formulae given elsewhere<sup>12</sup> which are more appropriate than (11) for this purpose. However, approximations are used by the code which limit the maximum admissible betatron phase-shift between the head and the tail of the bunch to 5 rad.

A rule of thumb for suppressing transverse coupled-bunch modes is that the rms spread in the frequency  $Q \cdot \omega_0$ , somewhat different for each bunch, should exceed the growth rate  $\text{Im}(\Delta\omega_{mn})$ . Since this spread arises from the difference in bunch populations via the Laslett tune-shifts caused by the ac fields only<sup>14,15</sup>, these tune-shifts are calculated by the program so that the spread in the bunch populations required to achieve the decoupling may be estimated.

### 5. Turbulent Bunch-Lengthening

It is assumed that turbulent bunch-lengthening is caused by the same microwave instability as occurs in proton machines<sup>16</sup>. Adapting the formulae to electron machines yields for the equilibrium rms, energy spread  $\delta_E$ ,

$$\delta_E^2 = \frac{e I_0}{F \cdot E} \cdot \gamma_t^2 \cdot |Z_L(\omega)/r| \quad (13)$$

valid for  $\delta_E \geq \delta_{E0}$  where  $\delta_{E0}$  is the spread for vanishing intensity. The form factor  $F$  is about 6 for a Gaussian distribution in energy. Inserting from (3) for the peak current and eliminating  $\delta_E$  by means of  $\delta_E = (Q_s \cdot \gamma_t^2) \cdot (\sigma_s/R)$  yields for the equilibrium bunch length  $\sigma_s$

$$\left( \frac{\sigma_s}{R} \right)^3 = \frac{\sqrt{2\pi} e I_0}{F k_b \gamma_t^2 Q_s^2 E} \cdot \left| \frac{Z_L(\omega)}{r} \right| \quad (14)$$

This equation also defines either the threshold current

for a given impedance, or the threshold impedance if the current is given; in both cases,  $\sigma_s$  must be replaced by the natural bunch length  $\sigma_{s0}$ . For the computation of  $\sigma_s$  for given  $I_0$  and  $Z_L/r$ , the SPEAR-type<sup>4</sup> broad-band impedance (section 2.1) is used in the program. Thus, for low frequencies

$$|Z_L/r| = Z_a (\omega_0/\omega_a) \quad \omega \leq \omega_a \quad (15a)$$

independent of  $\omega$ ; for high frequencies

$$|Z_L/r| = Z_a (\omega_0/\omega_a) \cdot (\omega/\omega_a)^{a-1} \quad \omega \geq \omega_a \quad (15b)$$

where  $Z_a$ ,  $\omega_a$  and  $a$  are constants. In order to obtain a numerical value from (15b) a typical frequency  $\omega = \omega_c$  must be selected. If  $\omega_c = c/\sigma_s$  is used in (15b) and the latter introduced into (14), the scaling law<sup>4</sup>, describing the observed bunch-lengthening in SPEAR II very well, is obtained. The program calculates, for both values of  $|Z/r|$  given by (15), the threshold current and in addition, if the threshold is exceeded, the new equilibrium values for bunch length, energy spread and peak current. The result obtained with (15a) should be used for long bunches; the results based on (15b) should be preferred for short bunches. Bunch lengthening by potential well distortion is neglected as it is always small for realistic impedances<sup>17</sup>.

## 6. Program Structure

The program requires as input only a few basic parameters of the accelerator and information on the natural beam dimensions. The code computes the effects sequentially starting with turbulent bunch-lengthening and Laslett tune-shifts. The user has the choice of retaining for further calculation either the natural bunch dimensions or the equilibrium values after turbulence. The main part of the program is concerned with coherent bunch motion. For the longitudinal bunch oscillation, the combined effect of up to three resonators (RF, broad-band, narrow-band parasitic) can be evaluated. The program computes the complex shift  $\Delta\omega_{mn}$  (8), and it can search for the most unfavourable tuning of the narrow-band resonator. Landau damping from the non-linearity of a perfect RF waveform is estimated. For transverse bunch oscillations two resonators can be taken into account, a high-Q one and a low-Q one. The complex frequency shifts  $\Delta\omega_{mn}$  (10) and  $\Delta\omega_m$  (12) are calculated for each of the resonators separately as well as for their combined effect. The effect of the smooth, resistive pipe on transverse bunch oscillations is computed for the head-tail (shape) modes  $m = 0,1$  neglecting its contribution above the cut-off frequency of the pipe.

## 7. Example

The program has been used extensively to study beam stability in the 3.5 km radius version of LEP<sup>18</sup> for a variety of operating conditions. The following numerical results<sup>18</sup> refer to the nominal LEP energy of 70 GeV. The longitudinal low-Q impedance is obtained by averaging the resistive impedance of the parasitic TM modes in the RF cavities over 250 MHz bins and adding to this the impedance of the chamber. The latter is described by (15) with  $a = 0.32$ ,  $\omega_a/2\pi = 1.3$  GHz and  $Z_a = 0.17$  M $\Omega$ , which is the SPEAR II impedance<sup>4</sup> except that  $Z_a/2R\pi$  is reduced by a factor 5 to take into account the smoother vacuum chamber of LEP. The resulting histogram (Fig. 2) is approximated by an impedance (15b) with  $a = 0.32$ ,  $\omega_a/2\pi = 1.3$  GHz and  $Z_a = 0.56$  M $\Omega$  for the calculation of bunch lengthening. The latter indicates that the natural bunch length ( $\sigma_{s0} = 1.3$  cm) and energy spread will increase by about a factor 4 in LEP because the design current (11 mA) exceeds the threshold current (1.2 mA). For computation of long-bunch stability the histogram is approximated by a resonator of  $Q_r = 1$ ,  $f_r = 1.3$  GHz and  $R_s = 0.56$  M $\Omega$  as shown

in Fig. 2. The lowest parasitic TM mode ( $f_r = 525$  MHz) of the RF cavities is selected to represent the typical narrow-band resonator. Taking into account dimensional tolerances on the cavities results in  $Q_r \approx 3000$  and  $R_s \approx 450$  M $\Omega$ . The computation of frequency shifts (8) with these two resonators shows that all growth rates are small compared to radiation damping ( $\tau = 6$  ms). However, if the RF fundamental is added, a few coupled-bunch modes having frequencies in the RF bandwidth become very strong and a feedback system becomes imperative.

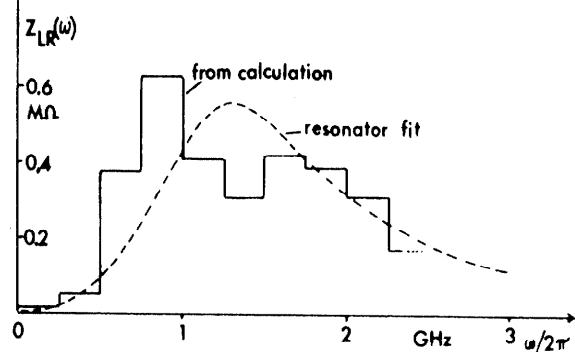


Fig. 2. Estimated resistive longitudinal broad-band impedance and approximation by a  $Q_r = 1$  resonator.

In order to obtain parameters for a typical high-Q transverse impedance, the lowest deflecting mode ( $f_r = 565$  MHz) of the RF cavities is calculated<sup>6</sup>. Due to consideration of the spread in  $f_r$  gives  $Q_r \approx 3000$  and  $R_T = 4.8$  G $\Omega$ /m. The low-Q impedance is obtained from the long one by means of (2) yielding  $f_r = 1.3$  GHz,  $Q_r = 1$  and  $R_T = 4.6$  M $\Omega$ /m. As in the longitudinal case, the coupled-bunch modes have a small growth-rate due to the wide spacing of the four bunches, but for non-zero chromaticity a single-bunch head-tail instability becomes strong indicating the importance of a close chromaticity control in LEP.

## Acknowledgement

The authors would like to thank Miss P.M. Hanney for writing the program and assistance during testing.

## References

1. W. Schnell, contribution to this conference.
2. E. Keil, Nucl. Instr. Meth. **100**, 419, 1972.
3. K. Halbach, R.F. Holsinger, Part. Acc. **7**, 213, 1976.
4. P.B. Wilson, R. Servranckx, A.P. Sabersky, J. Gareyte, G.E. Fischer, A.W. Chao, M.H.R. Donald, IEEE Trans. Nucl. Sci., **NS-24**, 1211, 1977.
5. F.J. Sacherer, Proc. 9th Internat. Conf. on High Energy Accelerators, Stanford, 347, 1974.
6. B. Zotter, CERN Internal Report, ISR/TH/70-52, 1970.
7. W. Schnell, CERN Internal Report, ISR-RF/70-7, 1970.
8. D. Möhl, CERN Internal Report MPS/DL/Note 72-6, 1972.
9. F.J. Sacherer, IEEE Trans. Nucl. Sci., **NS-20**, 825, 1973.
10. F.J. Sacherer, IEEE Trans. Nucl. Sci., **NS-24**, 1393, 1977.
11. J. Gareyte, Report SPEAR 206, 1977.
12. F.J. Sacherer, in Report CERN 77-13, 198, 1977.
13. B. Zotter, CERN Internal Report ISR-TH/78-16, 1978.
14. D. Möhl, Report LBL-570, 1971.
15. E. Brouzet, R. Cappi and J. Gareyte, CERN Internal Report, PS/OP/DL 78-14, 1978.
16. D. Boussard, CERN Internal Report, LAB. II/RF-int/75-2, 1975.
17. A. Hofmann, F. Pedersen, contribution to this conference.
18. LEP Study Group, CERN Internal Report, ISR-LEP/78-17, 1978.